Appendix: Rough Sets and Stomped Normal Distribution for Simultaneous Segmentation and Bias Field Correction in Brain MR Images

Abhirup Banerjee and Pradipta Maji

***Abstract*—The segmentation of brain MR images into different tissue classes is an important task for automatic image analysis technique, particularly due to the presence of intensity inhomogeneity artifact in MR images. In this regard, the paper presents a novel approach for simultaneous segmentation and bias field correction in brain MR images. It integrates judiciously the concept of rough sets and the merit of a novel probability distribution, called stomped normal (SN) distribution. The intensity distribution of a tissue class is represented by SN distribution, where each tissue class consists of a crisp lower approximation and a probabilistic boundary region. The intensity distribution of brain MR image is modeled as a mixture of finite number of SN distributions and one uniform distribution. The proposed method incorporates both the expectation-maximization and hidden Markov random field frameworks to provide an accurate and robust segmentation. The performance of the proposed approach, along with a comparison with related methods, is demonstrated on a set of synthetic and real brain MR images for different bias fields and noise levels.**

***Index Terms*—Segmentation, MRI, bias field, rough sets, expectation-maximization, hidden Markov random field.**

I. Experimental Results

A. Parameter Estimation of SN Distribution

Table I presents the estimated parameters μ, σ, and k for tissue classes grey matter (GM) and white matter (WM). The non-zero value of k implies that the algorithm applies stomped normal (SN) distribution to represent the tissue class, instead of Gaussian distribution ($k = 0$).

TABLE I
Mean (μ), Standard Deviation (σ), and Width (k) Parameter for all Images of BrainWeb and IBSR Database

Vol.	GM			WM		
No.	Mean	sd	k	Mean	sd	k
0-0	4.691	0.085	0.193	4.979	0.032	0.047
0-20	4.642	0.086	0.145	4.937	0.037	0.083
0-40	4.594	0.089	0.110	4.892	0.043	0.095
1-0	4.678	0.085	0.173	4.968	0.034	0.085
1-20	4.640	0.086	0.149	4.934	0.037	0.088
1-40	4.587	0.089	0.119	4.886	0.044	0.090
3-0	4.617	0.089	0.115	4.906	0.045	0.109
3-20	4.588	0.091	0.120	4.883	0.046	0.098
3-40	4.560	0.096	0.109	4.862	0.051	0.095
5-0	4.617	0.103	0.073	4.902	0.060	0.078
5-20	4.556	0.104	0.132	4.848	0.058	0.068
5-40	4.523	0.105	0.104	4.822	0.061	0.098
7-0	4.549	0.114	0.094	4.847	0.076	0.097
7-20	4.559	0.112	0.102	4.858	0.076	0.096
7-40	4.500	0.117	0.092	4.805	0.076	0.094
9-0	4.508	0.132	0.091	4.814	0.092	0.098
9-20	4.518	0.128	0.093	4.825	0.091	0.089
9-40	4.478	0.129	0.086	4.786	0.089	0.100
1	4.411	0.101	0.250	4.664	0.067	0.000
2	4.257	0.095	0.107	4.504	0.047	0.135
3	3.887	0.123	0.000	4.200	0.080	0.183
5	4.312	0.098	0.043	4.577	0.046	0.036
8	3.615	0.225	0.074	4.115	0.072	0.105
9	3.810	0.188	0.084	4.263	0.066	0.085
10	3.516	0.214	0.080	4.037	0.067	0.083
13	4.091	0.110	0.250	4.393	0.086	0.037
14	3.714	0.113	0.118	4.065	0.061	0.098
17	3.882	0.100	0.114	4.166	0.074	0.095

B. Importance of Rough Sets

To establish the importance of rough sets for simultaneous segmentation and bias field correction, experimentation is carried out on several images. The results are reported in Table III using rough sets (RS) and without using rough sets (NRS), with respect to RMSE and IoV indices. From the results reported in Table III for BrainWeb database, it is seen that the proposed algorithm using rough sets attains better restoration than its nonrough sets counter part in 15 cases out of total 18 cases with respect to the both RMSE and IoV values. In all other cases, its performance is comparable with the optimum result.

The comparative performance analysis is also reported in terms of p-value computed through Wilcoxon signed-rank test (one-tailed). The proposed method with rough sets attains lower p-values for all quantitative indices with respect to nonrough sets counter part, which are statistically significant considering 0.05 as the level of significance. Hence, all the results reported in Table III establish the importance of using rough sets in terms of bias field correction.

C. Performance of Different Bias Field Correction Algorithms

To find out the effectiveness of the proposed algorithm (StoRM) [1] for bias field correction over other existing algorithms such as RC2 [2], N3 [3], SPM [4], FSL [5], MICO [6], and the methods of Wells et al. [7], Guillemaud and Brady (GB) [8], and Zhang et al. [9], experimentation is carried out on eighteen images of BrainWeb, and the corresponding results are reported in Table II with respect to two quantitative indices. The Wilcoxon signed-rank test is also performed for significance analysis.

The authors are with the Biomedical Imaging and Bioinformatics Lab, Machine Intelligence Unit, Indian Statistical Institute, Kolkata, India. E-mail: {abhirup_r,pmaji}@isical.ac.in.

This work is partially supported by the Indian National Science Academy, New Delhi (grant no. SP/YSP/68/2012).

TABLE II
BIAS CORRECTION PERFORMANCE OF DIFFERENT ALGORITHMS WITH RESPECT TO RMSE AND IOV VALUES ON BRAINWEB DATABASE

Vol.	RMSE									IoV								
No.	StoRM	RC2	N3	SPM	FSL	Wells	GB	Zhang	MICO	StoRM	RC2	N3	SPM	FSL	Wells	GB	Zhang	MICO
0-0	0.12	2.03	8.24	3.39	70.82	1.04	1.29	0.12	5.24	0.999	0.986	0.987	0.998	0.833	0.984	0.979	0.999	0.992
0-20	4.73	3.77	9.03	3.17	69.30	4.24	4.06	4.67	4.49	0.962	0.965	0.987	0.995	0.852	0.963	0.962	0.962	0.929
0-40	9.21	8.79	8.31	4.16	69.51	8.45	8.23	9.00	13.70	0.927	0.937	0.985	0.997	0.856	0.950	0.948	0.931	0.937
1-0	0.32	2.01	7.44	5.63	66.41	1.07	1.25	0.32	5.10	0.999	0.984	0.992	0.983	0.820	0.984	0.981	0.999	0.995
1-20	4.49	3.70	8.62	3.85	67.59	4.13	4.01	4.41	9.50	0.959	0.963	0.990	0.985	0.839	0.960	0.959	0.962	0.937
1-40	8.85	8.41	7.62	6.70	68.12	8.11	7.93	8.60	6.33	0.924	0.939	0.991	0.989	0.855	0.950	0.948	0.929	0.928
3-0	0.15	1.82	3.48	5.12	62.40	1.00	1.15	0.65	4.88	0.999	0.986	0.995	0.982	0.826	0.986	0.985	0.997	0.997
3-20	6.04	5.79	6.47	6.10	62.22	5.96	5.93	5.94	6.55	0.971	0.969	0.996	0.982	0.859	0.965	0.965	0.976	0.927
3-40	7.48	13.98	7.14	6.44	61.35	7.02	6.93	7.24	10.84	0.939	0.682	0.989	0.980	0.881	0.957	0.955	0.947	0.888
5-0	0.37	14.74	4.59	5.27	54.01	1.15	1.27	2.33	4.85	0.998	0.709	0.997	0.984	0.840	0.987	0.986	0.994	0.998
5-20	8.79	14.52	8.75	9.09	53.72	8.82	8.79	8.74	8.39	0.974	0.707	0.982	0.975	0.886	0.975	0.975	0.975	0.901
5-40	9.74	9.71	11.78	8.73	58.03	9.53	9.48	9.41	11.68	0.957	0.959	0.979	0.969	0.852	0.967	0.967	0.962	0.944
7-0	1.52	1.57	5.71	6.29	52.00	1.55	1.67	5.17	5.14	0.996	0.987	0.997	0.983	0.874	0.986	0.984	0.994	0.998
7-20	11.86	11.78	12.41	12.43	53.63	11.85	11.88	13.41	10.53	0.972	0.977	0.986	0.969	0.890	0.971	0.970	0.968	0.952
7-40	12.09	12.18	15.73	12.08	53.22	12.04	11.98	12.11	10.03	0.967	0.970	0.981	0.973	0.874	0.973	0.970	0.956	0.947
9-0	3.46	1.48	4.87	7.30	47.33	3.87	2.35	87.62	5.61	0.995	0.987	0.994	0.986	0.907	0.987	0.985	0.904	0.991
9-20	15.04	14.46	14.58	15.39	50.44	14.98	14.78	23.18	12.20	0.972	0.978	0.979	0.974	0.902	0.970	0.967	0.973	0.973
9-40	14.39	14.27	16.79	14.83	49.21	14.43	14.21	19.54	13.49	0.970	0.978	0.963	0.964	0.897	0.966	0.963	0.968	0.977
p-value		*0.2754*	1.2E-03	*0.1733*	3.8E-06	**0.6491**	**0.9018**	*0.2850*	2.7E-02		*0.1419*	**0.9962**	**0.8481**	3.8E-06	*0.3830*	*0.2754*	**0.6475**	1.1E-02

TABLE III
PERFORMANCE OF PROPOSED ROUGH SET BASED ALGORITHM OVER BRAINWEB DATABASE

Vol.	RMSE		IoV	
No.	RS	NRS	RS	NRS
0-0	0.116	0.116	0.999	0.999
0-20	4.731	4.883	0.962	0.960
0-40	9.213	9.463	0.927	0.924
1-0	0.317	0.317	0.999	0.999
1-20	4.489	4.538	0.959	0.958
1-40	8.852	8.975	0.924	0.923
3-0	0.151	4.207	1.000	0.994
3-20	6.045	5.864	0.971	0.973
3-40	7.480	7.300	0.939	0.942
5-0	3.022	8.355	0.994	0.991
5-20	8.782	9.380	0.974	0.976
5-40	9.754	9.375	0.957	0.956
7-0	1.472	17.457	0.996	0.948
7-20	11.843	17.330	0.972	0.922
7-40	12.095	19.874	0.967	0.955
9-0	3.330	16.936	0.995	0.936
9-20	14.974	18.820	0.972	0.916
9-40	14.340	19.455	0.970	0.919
p-value	3.9E-03		3.3E-03	

From the results reported in last row of Table II, it can be seen that the proposed StoRM algorithm provides significantly better restoration than N3, FSL, and MICO with respect to RMSE value, considering 0.05 as the level of significance. The performance of StoRM is better, but not significantly (marked in italics) than RC2, SPM8, and the method of Zhang et al. [9] for RMSE, whereas the method proposed by Wells et al. [7] and Guillemaud and Brady (GB) [8] provide better but not significant (marked in bold) restoration performance than the StoRM. The performance of StoRM is again significantly better than FSL and MICO for IoV values. On the other hand, StoRM achieves better results, but not significant (marked in italics), compared to RC2 and the methods of Wells et al. [7] and Guillemaud and Brady (GB) [8] with respect to IoV index. However, SPM and the method proposed by Zhang et al. [9] provide better but not significant (marked in bold) restoration performance than the StoRM for IoV index, whereas N3 performs significantly better performance than StoRM with respect to IoV.

Fig. 1-4 compares the reconstructed images produced by the StoRM, RC2, N3, SPM, FSL, methods of Wells et al., Guillemaud and Brady, Zhang et al., and MICO for different bias fields, noise levels, and volumes. All the results reported in Fig. 1-4 establish the fact that the proposed StoRM algorithm estimates the bias field more accurately and restores images better than do the existing methods.

D. Performance of Different Segmentation Algorithms

This section compares the segmentation performance of the proposed StoRM algorithm with that of several existing algorithms, namely, SPM [4], FSL [5], MICO [6], KFLM [10], and the methods of Wells et al. [7], Guillemaud and Brady (GB) [8], and Zhang et al. [9].

Fig. 5-8 depicts the comparative segmentation performance of different algorithms considering some images. Corresponding original images and the ground truth images are also presented. The segmented outputs generated by different methods establish the fact that the proposed method generates more promising outputs that do the existing algorithms.

REFERENCES

[1] A. Banerjee and P. Maji, “Rough Sets and Stomped Normal Distribution for Simultaneous Segmentation and Bias Field Correction in Brain MR Images,” *IEEE Trans. on Image Processing (under revision)*.

[2] A. Banerjee and P. Maji, “Rough Sets for Bias Field Correction in MR Images Using Contraharmonic Mean and Quantitative Index,” *IEEE Trans. on Medical Imaging*, vol. 32, no. 11, pp. 2140–2151, 2013.

[3] J. G. Sled, A. P. Zijdenbos, and A. C. Evans, “A Nonparametric Method for Automatic Correction of Intensity Nonuniformity in MRI Data,” *IEEE Trans. on Medical Imaging*, vol. 17, no. 1, pp. 87–97, 1998.

[4] J. Ashburner and K. J. Friston, “Unified Segmentation,” *NeuroImage*, vol. 26, no. 3, pp. 839–851, 2005.

[5] M. Jenkinson, C. F. Beckmann, T. E. Behrens, M. W. Woolrich, and S. M. Smith, “FSL,” *NeuroImage*, vol. 62, no. 2, pp. 782–790, 2012.

[6] C. Li, J. C. Gore, and C. Davatzikos, “Multiplicative Intrinsic Component Optimization (MICO) for MRI Bias Field Estimation and Tissue Segmentation,” *Magnetic Resonance Imaging*, vol. 32, pp. 913–923, 2014.

[7] W. M. Wells, W. E. L. Grimson, R. Kikins, and F. A. Jolezs, “Adaptive Segmentation of MRI Data,” *IEEE Trans. on Medical Imaging*, vol. 15, no. 8, pp. 429–442, 1996.

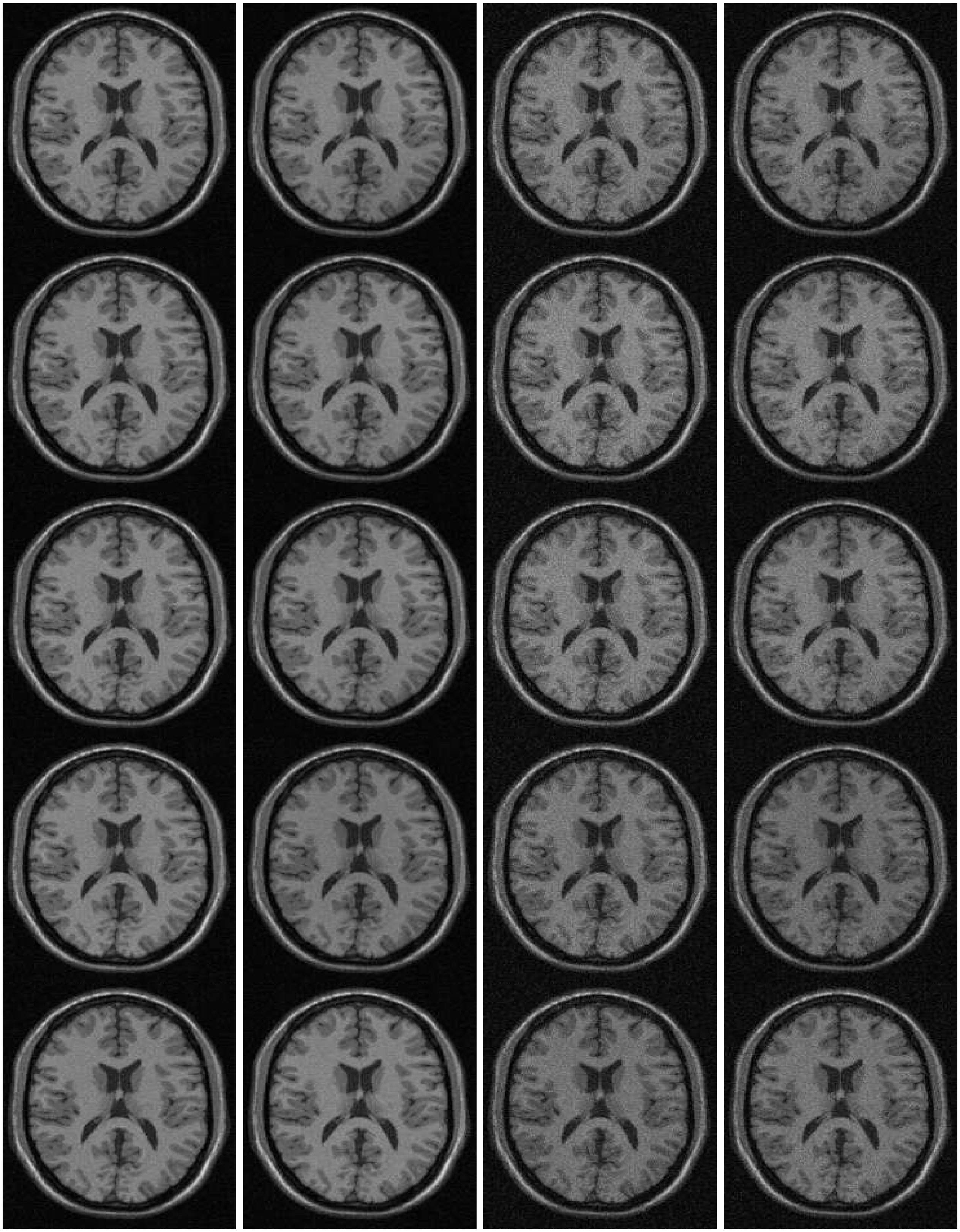

(a) 5-20 (b) 5-40 (c) 9-20 (d) 9-40

Fig. 1. Input and restored images of BrainWeb database by different algorithms: StoRM, RC2, N3, and SPM (top to bottom)

[8] R. Guillemaud and M. Brady, "Estimating the Bias Field of MR Images," *IEEE Trans. on Medical Imaging*, vol. 16, no. 3, pp. 238–251, 1997.

[9] Y. Zhang, M. Brady, and S. Smith, "Segmentation of Brain MR Images Through a Hidden Markov Random Field Model and the Expectation-Maximization Algorithm," *IEEE Trans. on Medical Imaging*, vol. 20, no. 1, pp. 45–57, 2001.

[10] M. Gong, Y. Liang, J. Shi, W. Ma, and J. Ma, "Fuzzy C-Means Clustering With Local Information and Kernel Metric for Image Segmentation," *IEEE Trans. on Image Processing*, vol. 22, no. 2, pp. 573–584, 2013.

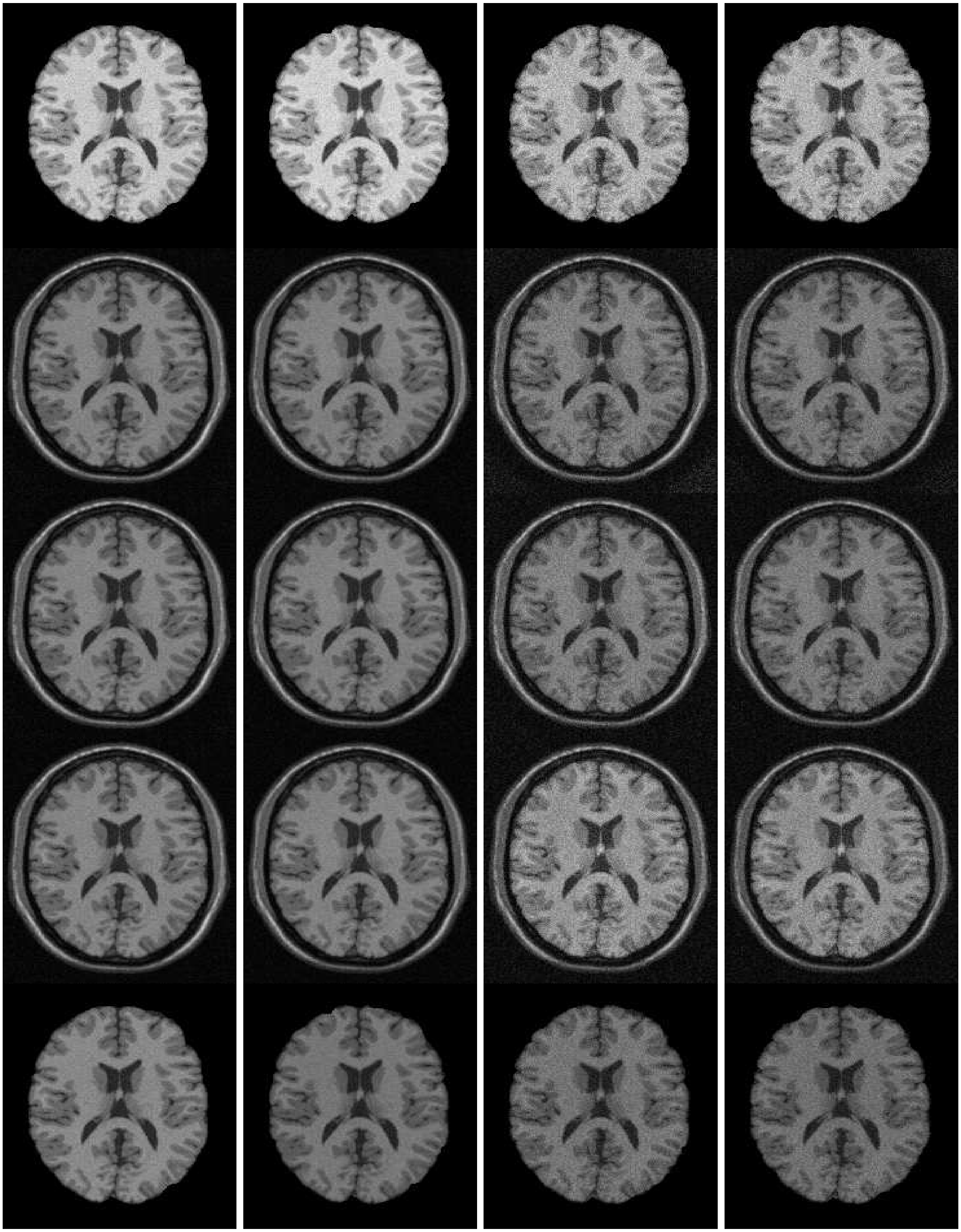

(a) 5-20 (b) 5-40 (c) 9-20 (d) 9-40

Fig. 2. Restored images of BrainWeb database by different algorithms: FSL, Wells, GB, Zhang, and MICO (top to bottom)

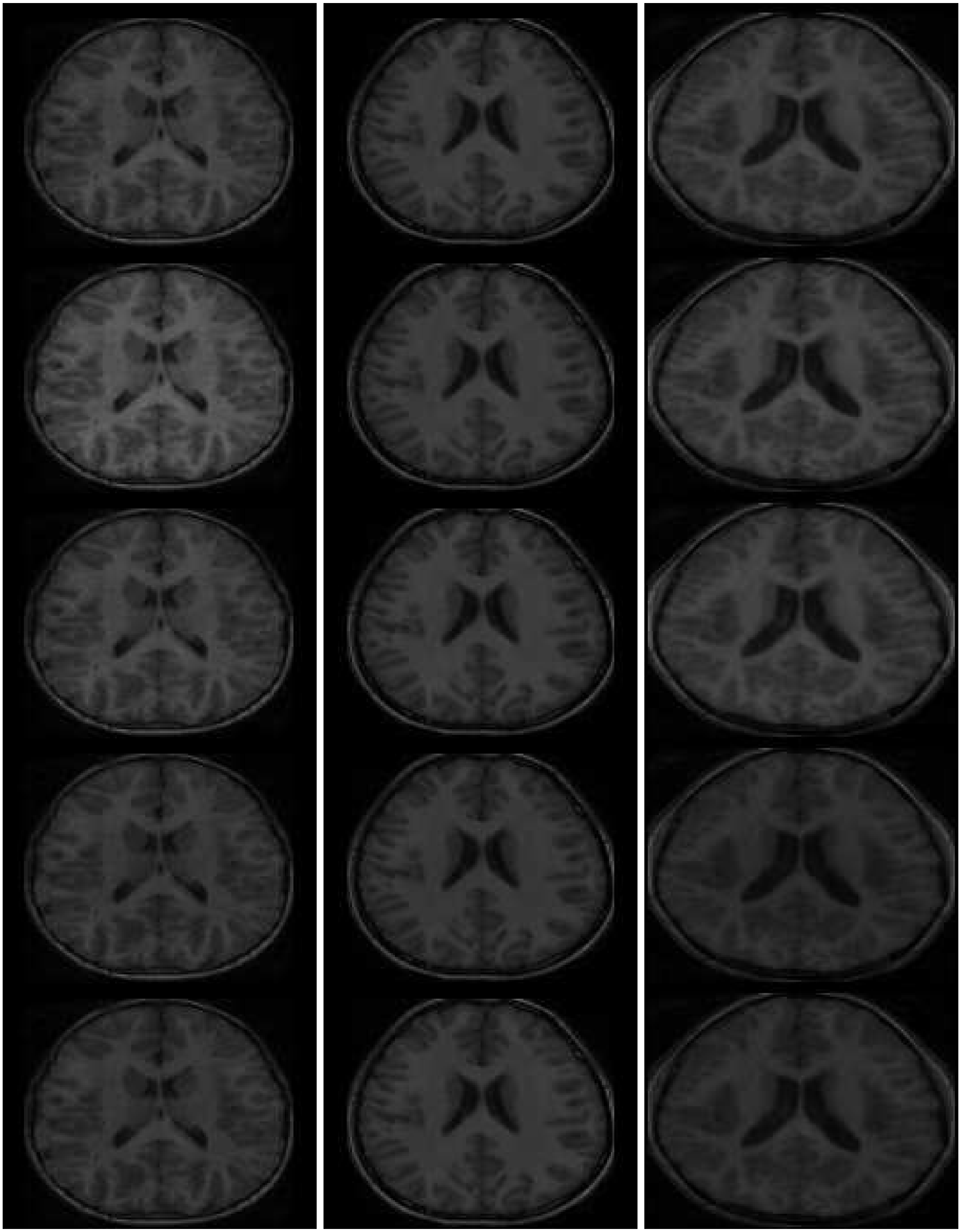

(a) V13 (b) V14 (c) V17

Fig. 3. Input and restored images of IBSR database by different algorithms: StoRM, RC2, N3, and SPM (top to bottom)

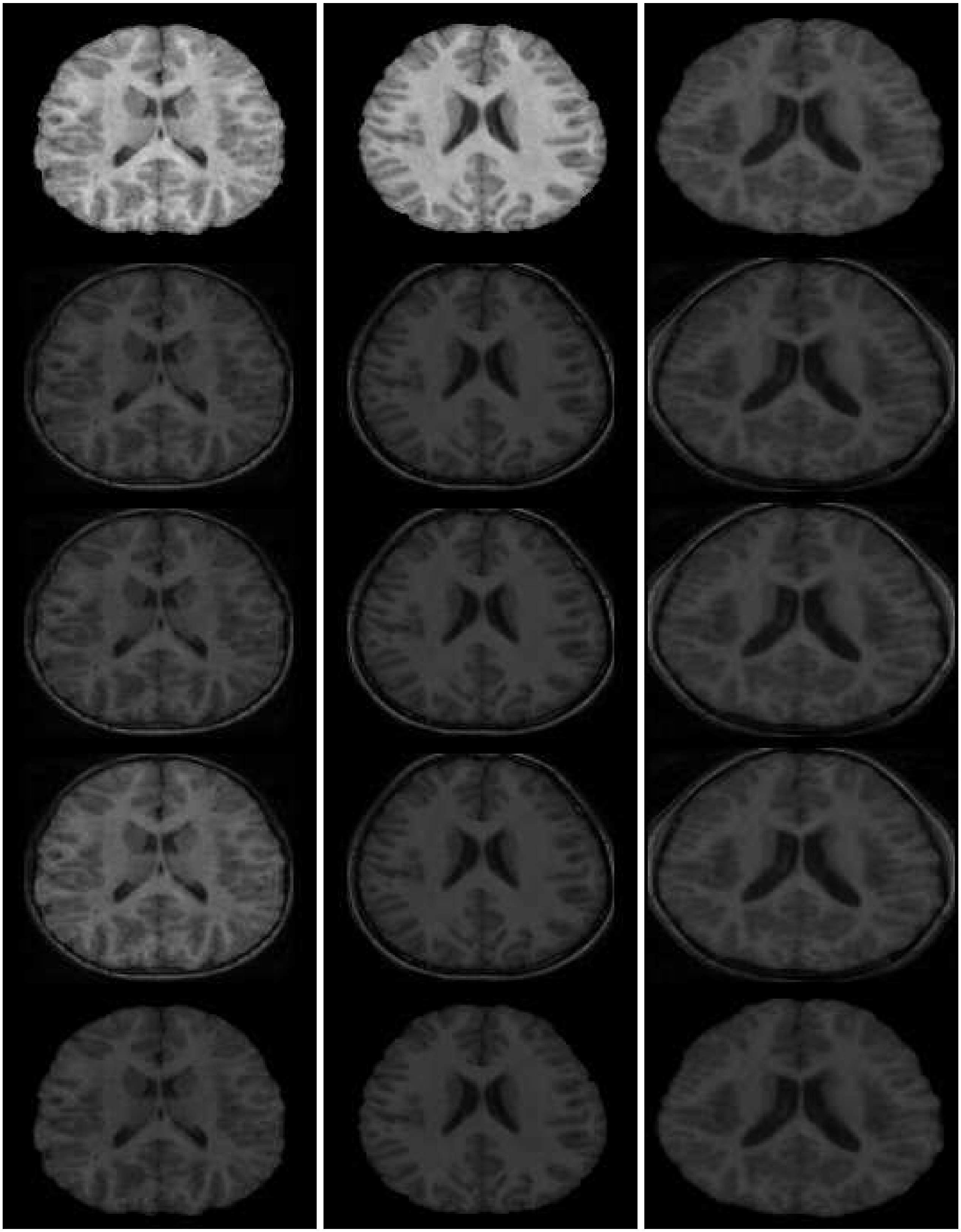

(a) V13 (b) V14 (c) V17

Fig. 4. Restored images of IBSR database by different algorithms: FSL, Wells, GB, Zhang, and MICO (top to bottom)

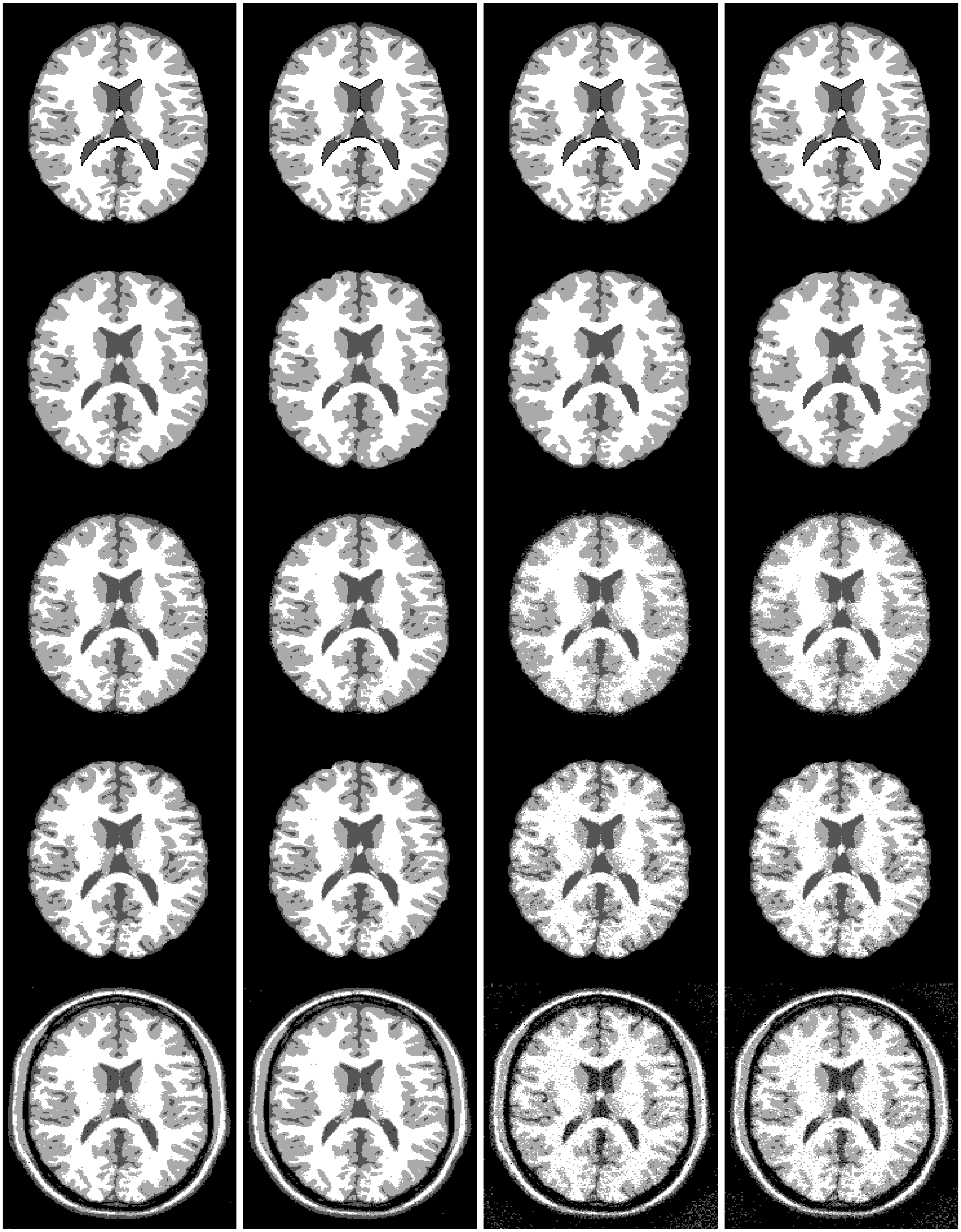

(a) 5-20 (b) 5-40 (c) 9-20 (d) 9-40

Fig. 5. Ground truth and segmented images of BrainWeb database using different algorithms: StoRM, SPM, FSL, and Wells (top to bottom)

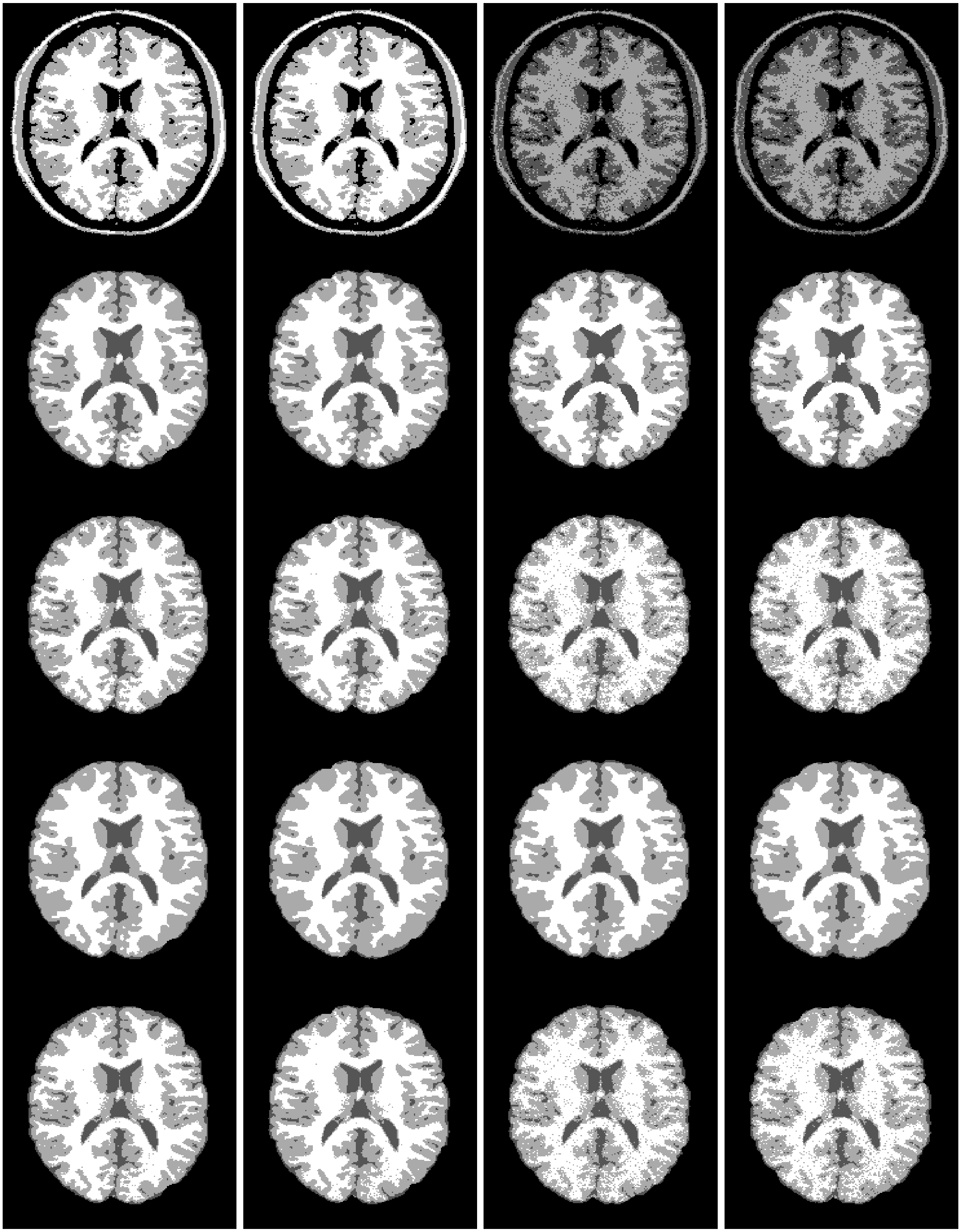

(a) 5-20 (b) 5-40 (c) 9-20 (d) 9-40

Fig. 6. Segmented images of BrainWeb database using different algorithms: GB, Zhang, MICO, KFLM, and RFCM (top to bottom)

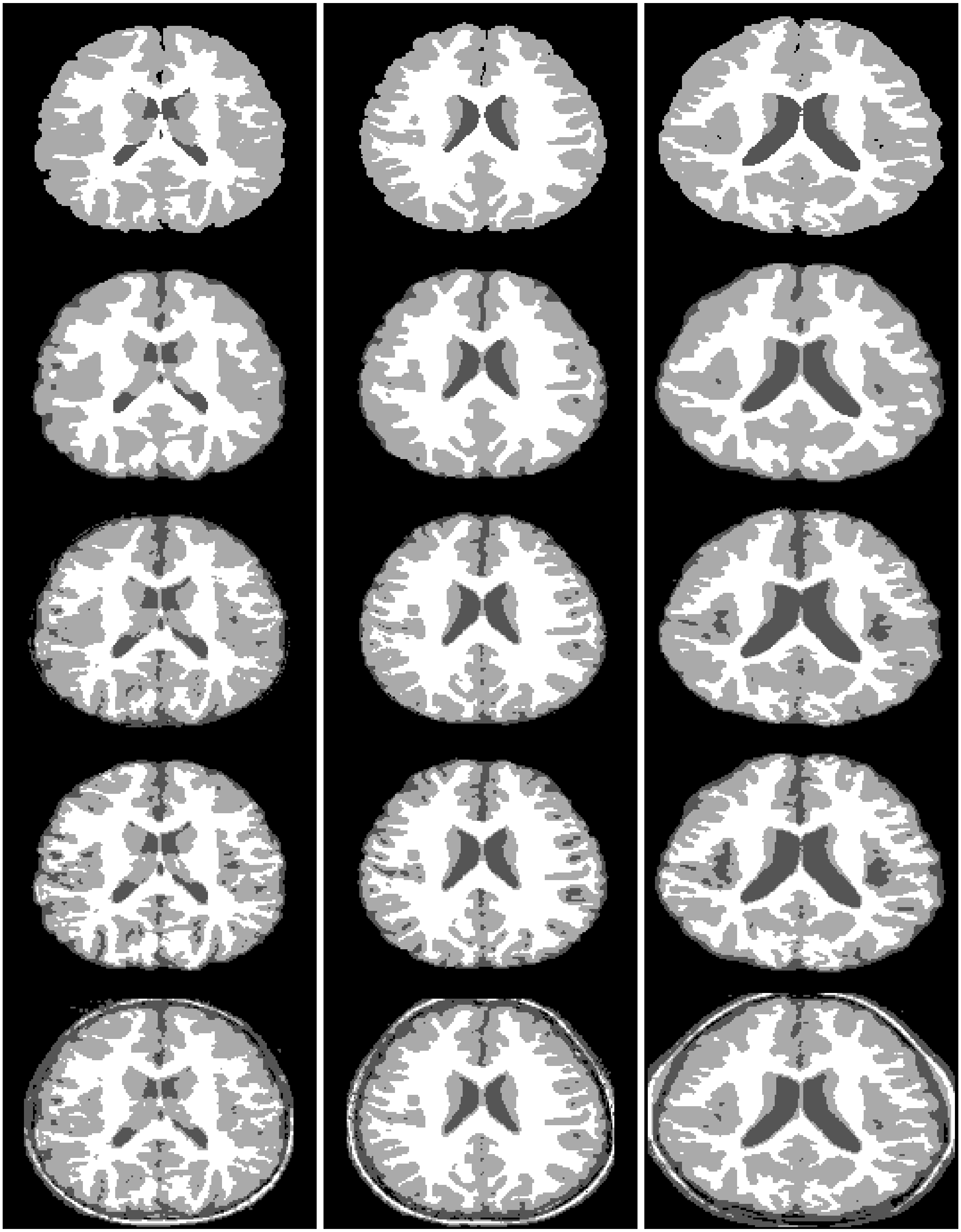

(a) V13 (b) V14 (c) V17

Fig. 7. Ground truth and segmented images of IBSR database using different algorithms: StoRM, SPM, FSL, and Wells (top to bottom)

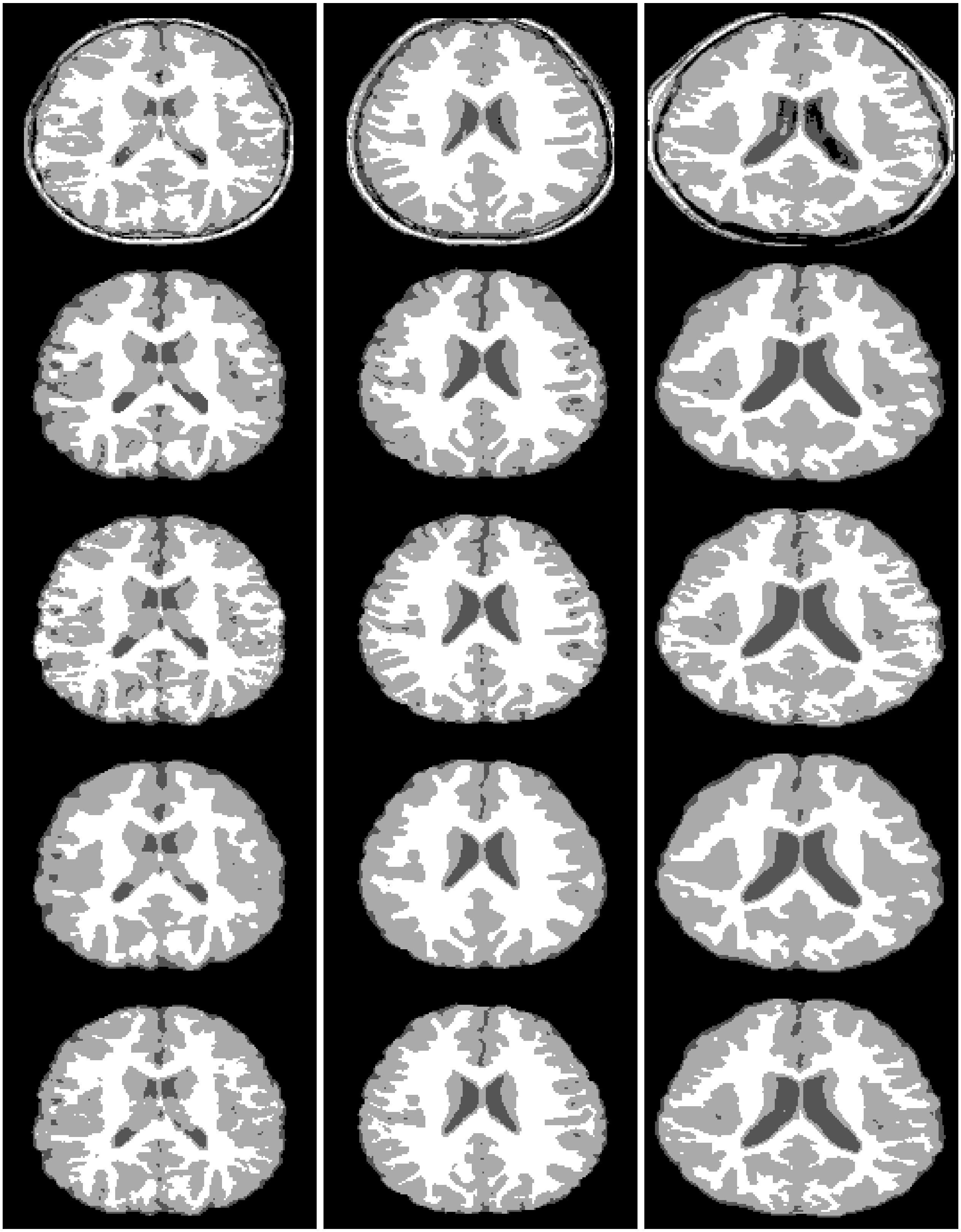

(a) V13 (b) V14 (c) V17

Fig. 8. Segmented images of IBSR database using different algorithms: GB, Zhang, MICO, KFLM, and RFCM (top to bottom)